Tetrahedron 68 (2012) 6193–6197

Contents lists available at SciVerse ScienceDirect

Tetrahedron

journal homepage: www.elsevier.com/locate/tet

Polyether-bridged bis(*tert*-butyl nitroxide) paramagnetic hosts showing receptor ability to calcium(II) and barium(II) ions

Sayaka Osada, Naoki Hirosawa, Takayuki Ishida *

Department of Engineering Science, The University of Electro-Communications, Chofu, Tokyo 182-8585, Japan

ARTICLE INFO

Article history:
Received 24 April 2012
Received in revised form 16 May 2012
Accepted 18 May 2012
Available online 26 May 2012

Keywords:
Radicals
Supramolecular chemistry
Host–guest systems
Exchange interaction
Electron spin resonance

ABSTRACT

The title compounds, Ph2bNO and Ph3bNO, were designed as a biradical paramagnetic host, and their chelation ability was confirmed by inclusion of a size-matched alkaline-earth metal ion. The crystal structures of [Ca(hfac)$_2$(Ph2bNO)] and [Ba(hfac)$_2$(Ph3bNO)] were determined, where Hhfac stands for 1,1,1,5,5,5-hexafluoropentane-2,4-dione. The solution electron paramagnetic resonance spectra showed switching behavior. Five lines were found for Ph3bNO and charecterized as the hyperfine splitting due to the two nitrogen atoms. After addition of barium(II) ion, the spectrum turned to be three lines. Removal of the barium ion recovered the five line pattern. The present system can be regarded as a reversible magnetic-coupling switch by means of a supramolecular technique.

1. Introduction

Supramolecular techniques, such as host-guest complex formation have been applied to tune molecule-based magnetic materials toward the development of information storage and molecular computing devices.[1] We have proposed and actually prepared several spin-labels, in which the paramagnetic centers, such as nitroxide (>N–O$^\bullet$) directly coordinated to the metal ion (M^{n+}) as a guest, thus affording an $O^\bullet$–M^{n+}–$O^\bullet$ superexchange pathway.[2] As Scheme 1 shows, the magnetic exchange coupling can be changed depending on the 'off' and 'on' states of the guest ions. The nitronyl nitroxide radical group (4,4,5,5-tetramethylimidazolin-1-oxyl 3-oxide)[3] has been the best investigated for metal-radical hybrid solids.[4] We are now focusing on aryl *tert*-butyl nitroxide derivatives,[5] because the nitroxide coordination has an advantage for the strong metal–radical exchange interaction in comparison with nitronyl nitroxide and related spin-delocalized radicals.[5,6]

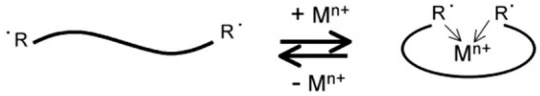

Scheme 1. Open and folded forms of bis(radical-armed) polyethers.

In this report we propose bis(*tert*-butyl nitroxide) compounds concatenated with polyether bridges; namely, PhnbNO with n=2 and 3 (Scheme 2). One may recall EGTA and BAPTA known as strong Ca^{2+} ion receptors[7] and suppose the possible utility for an ion sensor or imaging agent, which will be detectable by means of electron paramagnetic resonance (EPR) spectroscopy when the host is paramagnetic. We describe the structural and magnetic characterization and solution EPR analysis on the Ph2bNO, Ph3bNO, and their metal-ion complexes. The advantage of the EPR technique will be demonstrated in the study of subtle change of exchange interaction for well-separated biradical systems.[8]

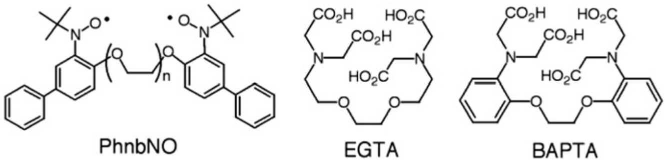

Scheme 2. Structural formulas of PhnbNO, EGTA, and BAPTA.

2. Results and discussion

2.1. Synthesis and characterization of the host compounds

Ph2bNO and Ph3bNO were prepared according to the conventional procedure.[5] Peripheral phenyl groups are introduced for the improvement of stability under ambient conditions. The compounds were purified by column chromatography and recrystallization.

---

* Corresponding author. Tel.: +81 42 443 5490; fax: +81 42 443 5501; e-mail address: ishi@pc.uec.ac.jp (T. Ishida).

0040-4020/$ – see front matter © 2012 Elsevier Ltd. All rights reserved.
doi:10.1016/j.tet.2012.05.065

The EPR spectrum of Ph2bNO showed five lines with $a_{N(-O)}=0.716$ mT at $g=2.0062$ (9.4 GHz in toluene at room temperature), being typical of bisnitroxide compounds (Fig. 1). Ph3bNO also showed five lines with $a_{N(-O)}=0.718$ mT at $g=2.0062$. The fast-exchange limit would show five lines while the slow-exchange limit three.[9] Even when the polyether bridge was longer (Ph4bNO etc.), five lines were still observed. No appreciable concentration dependence of the line-shape was observed below 10^{-4} mol L^{-1}. The exchange was supposed to occur in a through-space manner, because the nitroxide groups have a dipolar character ($>N^{+\bullet}-O^{-}$) favoring a head-to-tail dimerization.[10] In a dilute solution, the intramolecular nitroxide dimerization would take place with a flexible polyether backbone bent to form a loop conformation, as previously proposed for polymethylene-bridged bis(2,2,6,6-tetramethylpieridin-1-oxyl) systems.[11]

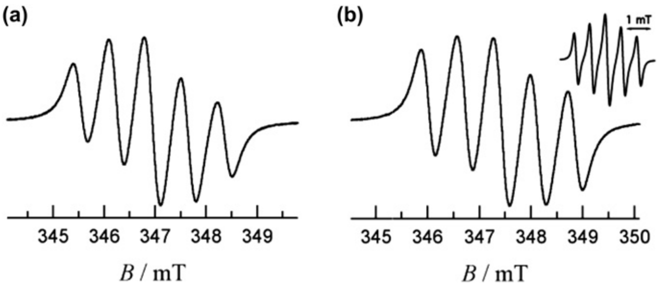

Fig. 1. X-Band EPR spectra of (a) Ph2bNO and (b) Ph3bNO in toluene at room temperature. The inset in (b) shows the spectrum of Ph3bNO measured at 380 K.

From a close look at the present spectra, we found that the relative intensity was considerably deformed from the ideal 1/2/3/2/1 hyperfine structure, suggesting the intermediate molecular motion rate with respect to the EPR timescale. This hypothesis was supported by variable-temperature EPR measurements; the intensity ratio approached the ideal pattern when the sample solution was heated to 107 °C in toluene (Fig. 1b, inset). Furthermore, the EPR line-shape showed solvent-dependence; the broadening of the second and fourth lines was clearly demonstrated in dichloromethane and chloroform (Supplementary data, Figs. S1 and S2).

The molar magnetic susceptibilities (χ_m) of polycrystalline samples of Ph2bNO and Ph3bNO were measured on a SQUID magnetometer. The data were analyzed on the empirical Curie–Weiss equation ($\chi_m=C/(T-\theta)$; C and θ stand for the Curie and Weiss constants, respectively). The constants were optimized as $C=0.78(2)$ cm^3 K mol^{-1} and $\theta=-2.61(7)$ K for Ph2bNO and $C=0.784(1)$ cm^3 K mol^{-1} and $\theta=-11.3(5)$ K for Ph3bNO. The spin-only values are expected as $C_{calcd}=0.75$ cm^3 K mol^{-1}, and accordingly the observed values imply the spin entity with a high purity. The negative θ values indicate the presence of antiferromagnetic interaction among the spins. The molecular structure of Ph3bNO was determined by means of X-ray crystallographic analysis (Fig. S3).

2.2. Synthesis and characterization of the host-guest complexes

We tried to prepare host-guest complexes of Ph2bNO and Ph3bNO with various metal ions, and eventually obtained good crystalline compounds [Ca(hfac)$_2$(Ph2bNO)] (**1**) and [Ba(hfac)$_2$(Ph3bNO)] (**2**), where Hhfac stands for 1,1,1,5,5,5-hexafluoropentane-2,4-dione. The effective ion radii of Ca^{2+} and Ba^{2+} are 1.00–1.34 and 1.35–1.61 Å,[12] respectively, and the successful combination suggests the importance of size-matching, though the hosts have an open chain structure.

As the X-ray diffraction study revealed (Fig. 2), **1** and **2** crystallize in orthorhombic $P2_12_12$ and orthorhombic $Pccn$ space groups, respectively, and half a molecule is crystallographically independent. Hosts Ph2bNO and Ph3bNO play the role of penta- and hexadentate ligands, respectively, as designed. The coordination numbers of the Ca^{2+} and Ba^{2+} ions are nine and ten, respectively. The two nitroxide oxygen atoms are coordinated to the metal center, with the $O^{\bullet}-M$ distances of 2.4558(18) Å for **1** and 2.767(3) Å for **2**. Note that the nitroxide oxygen atoms are somewhat closely located to each other with the $O^{\bullet}\cdots O^{\bullet}$ distances of 4.460(3) and 4.382(4) Å for **1** and **2**, respectively. The $O^{\bullet}-M-O^{\bullet}$ angles are 130.50(8) and 104.75(8)°, respectively.

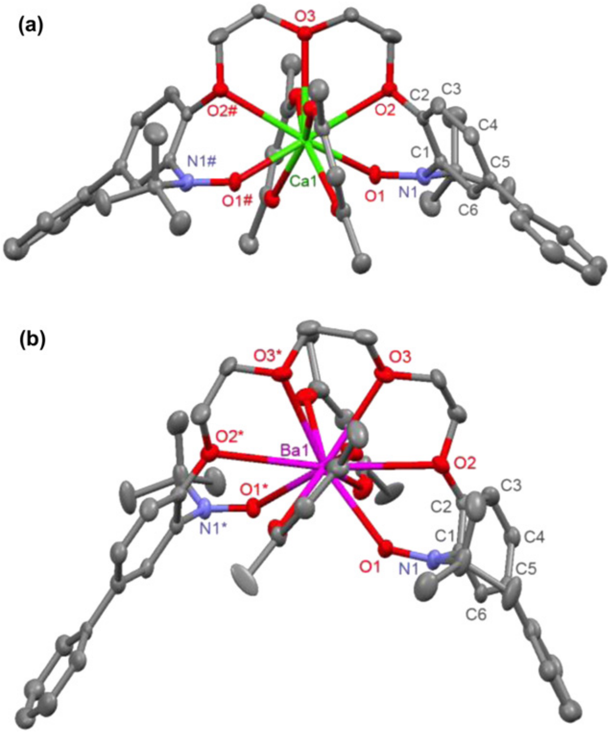

Fig. 2. X-ray crystal structures of (a) **1** and (b) **2**. Hydrogen and fluorine atoms are omitted. Thermal ellipsoids are drawn at the 50% probability level. Symmetry operation codes for # and * are ($-x$, $-y$, z) and ($-x+1/2$, $-y+1/2$, z), respectively.

The radical sites did not decompose during the complexation, as clarified by the spin entity determined by means of magnetic measurements (Fig. 3). The χ_mT values of **1** and **2** monotonically decreased on cooling. In these complexes, the hfac ligands magnetically insulate intermolecular interaction. The magnetic coupling parameter was estimated from the Bleaney–Bowers equation,[13] where the singlet-triplet energy gap is defined as $2J$. The optimized parameters are $2J/k_B=-1.51(2)$ K with $g=1.985(4)$ for **1** and $2J/k_B=-3.16(1)$ K with $g=1.986(3)$ for **2**. Assuming the g values of 2.006, the radical purities are estimated to be ca. 98% for both. The antiferromagnetic couplings were assigned to the $O^{\bullet}-M-O^{\bullet}$ superexchange together with a direct through-space $O^{\bullet}\cdots O^{\bullet}$ interaction. Similar interactions have been reported recently.[14,15]

2.3. EPR switching behavior

We measured solution EPR of the paramagnetic host in the presence of various metal ions, especially Ca^{2+} and Ba^{2+} ions. We found drastic change of the EPR line-shape for the combination of Ph3bNO and Ba(hfac)$_2$ in toluene (Fig. 4). The line became a three-line pattern just like a mononitroxide species (b). To eliminate the

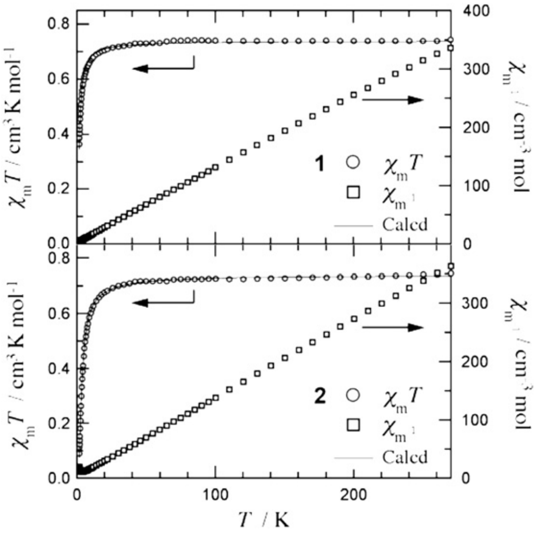

Fig. 3. Temperature dependence of $\chi_m T$ and χ_m^{-1} for **1** (top) and **2** (bottom). Solid lines represent calculated curves based on the singlet-triplet model. For the optimized parameters, see the text.

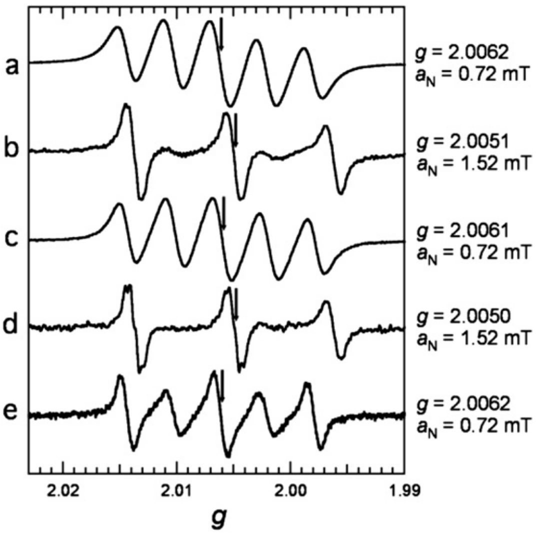

Fig. 4. EPR spectra of Ph3bNO in toluene at room temperature. The spectra were successively recorded in a sequence of (a) only Ph3bNO, (b) addition of 3 equiv of Ba(hfac)$_2$, (c) addition of 3 equiv of EGTA, (d) addition of 10 equiv of Ba(hfac)$_2$, and finally (e) addition of 10 equiv of EGTA. The EGTA addition was given as a solution in *N*,*N*-dimethylformamide. The arrows denote the signal center.

possibility of radical degradation, the Ba^{2+} ion was removed by addition of a stronger Ba^{2+} receptor, EGTA. The five-line shape was recovered (c), indicating that the host-guest association and dissociation are responsible for the reversible line-shape change. This change can be repeated a few times (d and e), but the signals finally became an intermediate and vague shape, because the solution is diluted and competing equilibria occur. The combination of Ca^{2+} and Ph2bNO exhibited a similar switching behavior of the EPR line shape, but it was somewhat complex owing to spectrum superposition.[16]

The hyperfine coupling constant (a_N) supports the complexation. The a_N value of the triplet signal is slightly larger than twice the a_N value of the quintet, indicating the larger contribution of a dipolar nature ($>N^{+\bullet}-O^-$) rather than a neutral one ($>N-O^\bullet$) in a coordination compound. The presence of a cation adjacent to the nitroxide oxygen atom emphasizes the dipolar-ionic bonding character.

The g value was also switched (Fig. 5a). The complexation with cation caused a slightly negative shift of the g value; namely, the metal-free Ph3bNO showed the five lines at g=2.0061(2) while the three lines appeared at g=2.0051(2) in the presence of Ba^{2+} ion. The positive charge of the species may the negative shift of the g values, as reported for various hydrocarbon anion and cation radicals.[17] The report on the g shift (Δg=0.000101) for the ascorbic acid radical anion before and after Ca^{2+} complexation[18] is a more closely related work. These g shifts are induced by decrease or increase of spin density on the radical oxygen or nitrogen atoms.

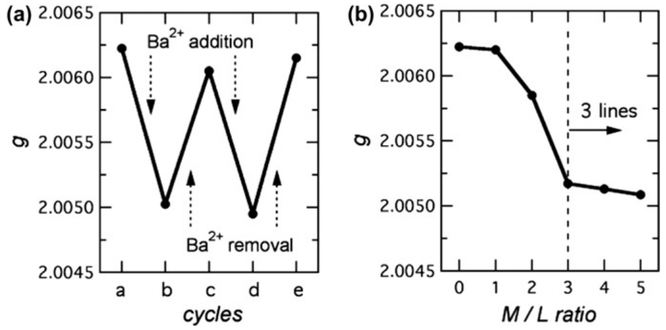

Fig. 5. (a) The g value in the experiment of the addition/removal of Ba^{2+} (see Fig. 4 for the conditions of a–e). (b) The g value as a function of the metal/ligand (M/L) ratio with the initial L concentration of 10^{-4} mol L^{-1}.

Though the presence or absence of the second and fourth lines is a convenient marker for the exchange coupling switch, the g-shift can also be easily monitored in the following EPR titration experiments (Fig. 5b). Addition of Ba^{2+} gradually changed the line shape and g value, and finally the addition of 3 equiv of Ba^{2+} completed the complexation. The result implies that the complexation equilibrium constant is not large. This argument is supported by the successful removal of Ba^{2+} ion with EGTA. The EGTA is a good Ba^{2+} chelater (association equilibrium constant, log K=8.32 in water), though it behaves as a much better Ca^{2+} chelater (log K=10.93 in water).[19] The present competition experiment implies that K between Ph3bNO and Ba^{2+} ion is smaller than that of EGTA and Ba^{2+} in toluene. From Fig. 5b, K is roughly estimated as log K=4–5.[20]

The fast exchange coupling unexpectedly disappeared for the Ph3bNO and Ba^{2+} complex. Ziessel and co-workers previously reported the lack of fast exchange coupling of the bis(nitronyl nitroxide) paramagnetic ligands after the complexation of diamagnetic ions, and explained this finding in terms of shielding of exchange.[21] A large guest cation provides a steric barrier that prevents coupling between the terminal radical centers and rotating in the flexible bridge. The present study has already revealed that an appreciable exchange occurs through the $O\bullet{-}M{-}O\bullet$ pathway (Figs. 2 and 3). Consequently we can assume a slightly different configuration in solution (ex. $O^\bullet\cdots M{-}O^\bullet$ or some high order structures). In other words, the dimerized nitroxide unit, which is present even at higher temperatures (Fig. 1), underwent facile dissociation by insertion of the metal ion.

3. Summary

We have developed PhnbNO (n=2, 3) as paramagnetic host compounds. They showed the geometrical change in the presence of a suitable ion in size, accompanied by the change of exchange coupling easily detectable in EPR.

One may wonder the inverse situation would be expected from Scheme 1; that is, a three-line pattern would have appeared before the complexation and the five-line pattern after. On the contrary, the observation is the other way round. The reason is the flexible loop conformation before complexation and the exchange-shielding after in a solution phase. The reversible magnetic-coupling switch has been established in this way, and this work can be regarded as a successful supramolecular control of organic/molecule-based magnetic properties. The flexible nature of the organic skeleton may play a key role in the application of organic magnetism.

4. Experimental section

4.1. Preparation of PhnbBr (*n*=2 and 3)

Precursory dibromides Ph2bBr and Ph3bBr (3-oxapentane-1,5-diyldioxy- and 3,6-dioxaoctane-1,8-diyldioxybis(2-bromo-4-phenylbenzene)s, respectively) were prepared from 2-bromo-4-phenylphenol[22] with diethylene and triethylene glycol tosylates, respectively, according to the Williamson procedure (by using potassium carbonate as a base in *N*,*N*-dimethylformamide; 120 °C, 18 h). Ph2bBr: yield, 76%. Mp 78–80 °C. ^{1}H NMR (500 MHz, $CDCl_3$) δ 7.77 (d, J=2 Hz, 2H), 7.50 (d, J=9 Hz, 4H), 7.45 (dd, J=9 Hz, 2 Hz, 2H), 7.40 (t, J=9 Hz, 4H), 7.32 (t, J=9 Hz, 2H), 7.00 (d, J=9 Hz, 2H), 4.27 (t, J=5 Hz, 4H), 4.09 (t, J=5 Hz, 4H). ^{13}C NMR (125.8 MHz, $CDCl_3$) δ 154.8, 139.5, 135.6, 132.0, 128.9, 127.3, 127.0, 126.8, 114.0, 112.9, 70.2, 69.5. Ph3bBr: yield, 86%. Mp 82–83 °C. ^{1}H NMR (500 MHz, $CDCl_3$) δ 7.77 (d, J=2 Hz, 2H), 7.50 (d, J=9 Hz, 4H), 7.44 (dd, J=9, 2 Hz, 2H), 7.40 (t, J=9 Hz, 4H), 7.32 (t, J=9 Hz, 2H), 6.97 (d, J=9 Hz, 2H), 4.23 (t, J=5 Hz, 4H), 3.96 (t, J=5 Hz, 4H), 3.85 (s, 4H). ^{13}C NMR (125.8 MHz, $CDCl_3$) δ 154.8, 139.4, 135.5, 132.0, 128.9, 127.3, 127.1, 126.8, 113.8, 112.8, 71.4, 69.7, 69.3.

4.2. Preparation of PhnbNO (*n*=2 and 3)

The hydroxylamines PhnbNOH (n=2 and 3) were prepared from the corresponding bromides by way of lithiation with butyl lithium in THF followed by coupling with 2-methyl-2-nitrosopropane. Ph2bNOH: yield, 79%. Mp 151–152 °C (decomp.). ^{1}H NMR (500 MHz, $(CD_3)_2SO$) δ 7.66 (d, J=2 Hz, 2H), 7.52 (d, J=8 Hz, 4H), 7.40 (t, J=8 Hz, 4H), 7.33 (dd, J=9, 2 Hz, 2H), 7.27 (t, J=8 Hz, 2H), 6.97 (d, J=9 Hz, 2H), 4.11 (t, J=5 Hz, 4H), 3.83 (t, J=5 Hz, 4H), 1.11 (s, 18H). ^{13}C NMR (125.8 MHz, $(CD_3)_2SO$) δ 152.9, 140.9, 140.6, 132.6, 129.5, 127.2, 126.6, 125.4, 124.3, 113.8, 69.8, 67.9, 60.8, 25.9. IR (neat, ATR (attenuated total reflectance)) 3201, 2972, 1486, 1135, 762 cm^{-1} Ph3bNOH: yield, 73%. Mp 152–153 °C (decomp.). ^{1}H NMR (500 MHz, $DCON(CD_3)_2$) δ 7.80 (d, J=2 Hz, 2H), 7.59 (d, J=8 Hz, 4H), 7.44 (t, J=8 Hz, 4H), 7.39 (dd, J=9, 2 Hz, 2H), 7.30 (t, J=8 Hz, 2H), 7.05 (d, J=9 Hz, 2H), 4.18 (t, J=5 Hz, 4H), 3.84 (t, J=5 Hz, 4H), 3.73 (s, 4H), 1.15 (s, 18H). ^{13}C NMR (125.8 MHz, $DCON(CD_3)_2$) δ 153.3, 141.0, 140.8, 132.8, 129.0, 126.8, 126.4, 125.4, 124.1, 114.3, 70.7, 69.8, 68.3, 60.7, 25.3. IR (neat, ATR) 3243, 2967, 1487, 1138, 759 cm^{-1}. The hydroxylamines were dissolved in dichloromethane (20 mL) and oxidized with freshly prepared Ag_2O.[23] Final products PhnbNO were purified by silica-gel column chromatography eluted with dichloromethane. A red fraction was collected and concentrated under a reduced pressure, giving red prisms. Ph2bNO: yield, 61%. Mp 122–123 °C. ESI-MS (methanol) m/z=605.3 (100%, M+Na$^+$), 621.2 (29%, M+K$^+$). Calcd 582.31 for $C_{36}H_{42}N_2O_5$. IR (neat, ATR) 2973, 1485, 1278, 1142, 765 cm^{-1}. EPR (rt in toluene) g=2.0062, a_N=0.716 mT (quintet). Anal. Found: C, 74.43; H, 7.28; N, 4.80%. Calcd: C, 74.20; H, 7.26; N, 4.81% for $C_{36}H_{42}N_2O_5$. Ph3bNO: yield, 85%. Mp 143–145 °C. ESI-MS (1/1 methanol/chloroform) m/z=649.3 (100%, M+Na$^+$), 665.3 (73%, M+K$^+$). Calcd 626.34 for $C_{38}H_{46}N_2O_6$. IR (neat, ATR) 2866, 1485, 1279, 1140, 769 cm^{-1}. EPR (rt in toluene) g=2.0062, a_N=0.718 mT (quintet). Anal. Found: C, 72.78; H, 7.20; N, 4.38%. Calcd: C, 72.82; H, 7.40; N; 4.47% for $C_{38}H_{46}N_2O_6$.

4.3. Preparation of Ca and Ba complexes

Complexation of Ph2bNO and $Ca(hfac)_2$ in a dichloromethane–heptane mixed solution gave red platelet crystals of $[Ca(hfac)_2(Ph2bNO)]$ (**1**) after the solvent was almost removed on warming below 90 °C. The yield was 43%. Mp 146–148 °C. Anal. Found: C; 53.58, H; 4.31, N, 2.76%. Calcd. C; 53.28, H; 4.28, N, 2.70% for $C_{46}H_{44}CaF_{12}N_2O_9$. IR (neat, ATR) 2940, 1673, 1533, 1147, 768 cm^{-1}. Complexation using Ph3bNO and $Ba(hfac)_2$ in a similar manner to that of **1** gave red prisms of $[Ba(hfac)_2(Ph3bNO)]$ (**2**) in 47% yield. Mp 161–164 °C. Anal. Found: C; 48.94, H; 3.81, N, 2.38%. Calcd: C; 48.93, H; 4.11, N, 2.38% for $C_{48}H_{48}BaF_{12}N_2O_{10}$. IR (neat, ATR) 2947, 1671, 1528, 1119, 766 cm^{-1}.

4.4. X-ray crystallographic analysis

X-ray diffraction data were collected on a Saturn70 CCD diffractometer with graphite monochromated MoKα radiation (λ=0.71073 Å). The structures were directly solved and expanded using Fourier techniques in the CRYSTALSTRUCTURE 4.0 program package.[24] Selected data for Ph3bNO: $C_{38}H_{46}N_2O_6$, monoclinic, $P2_1/c$, a=12.320(7), b=18.04(2), c=9.251(5) Å, β=125.945(7)°, V=1664(3) Å^3, Z=2, d_{calcd}=1.251 g cm^{-3}, μ(Mo$K\alpha$)=0.0840 mm^{-1}, R_{int}=0.042, $R(F)$ (I>2σ(I))=0.0488, $R_w(F^2)$ (all data)=0.1342, and T=90 K for 3797 unique reflections. Selected data for **1**: $C_{46}H_{44}CaF_{12}N_2O_9$, orthorhombic, $P2_12_12$, a=15.914(7), b=12.739(6), c=11.766(11) Å, V=2385(3) Å^3, Z=2, d_{calcd}=1.444 g cm^{-3}, μ(Mo$K\alpha$)=0.2338 mm^{-1}, R_{int}=0.058, $R(F)$ (I>2σ(I))=0.0565, $R_w(F^2)$ (all data)=0.0941, and T=100 K for 5461 unique reflections. Selected data for **2**: $C_{48}H_{48}BaF_{12}N_2O_{10}$, orthorhombic, $Pccn$, a=24.726(7), b=12.402(7), c=16.377(5) Å, V=5022(4) Å^3, Z=4, d_{calcd}=1.558 g cm^{-3}, μ(Mo$K\alpha$)=0.893 mm^{-1}, R_{int}=0.049, $R(F)$ (I>2σ(I))=0.0582, $R_w(F^2)$ (all data)=0.1739, and T=90 K for 5748 unique reflections. CCDC reference numbers 869280–869282.

4.5. Physical measurements

The dc magnetic susceptibilities of polycrystalline specimens of the present compounds were measured on a Quantum Design SQUID magnetometer (MPMS-7) in a range of 1.8–300 K. A static magnetic field of 5000 Oe was applied. The EPR spectra were obtained on a Bruker ESP300E spectrometer equipped with an X-band macrowave oscillator. The solution was degassed and measured at room temperature. Typical concentration was 10^{-4} mol L^{-1}.

Acknowledgements

This work was supported by Grants-in-Aids for Scientific Research (Nos. 23110711 and 22350059) from the Ministry of Education, Culture, Sports, Science and Technology, Japan. The authors thank Prof. Daisuke Shiomi and Dr. Yuki Kanzaki (Osaka City University) for fruitful discussion and Mr. Akira Nozawa (The Univ. of Electro-Communications) for assistance in the ESI-MS measurements.

Supplementary data

X-Band EPR spectra of Ph2bNO and Ph3bNO in dichloromethane and chloroform and X-ray crystal structures of Ph3bNO, $[Ca(hfac)_2(Ph2bNO)]$ (**1**), and $[Ba(hfac)_2(Ph3bNO)]$ (**2**). CCDC 869280, 869281, and 869282 contain the supplementary crystallographic data for Ph3bNO, **1**, and **2**, respectively. These data can be obtained free of charge from via http://www.ccdc.cam.ac.uk/conts/retrieving.html, or from the Cambridge Crystallographic Data Centre, 12 Union Road, Cambridge CB21 EZ, UK; fax: (+44) 1223-336-033; or e-mail: deposit@ccdc.cam.ac.uk. Supplementary data associated with this article can be found, in the online version, at doi:10.1016/j.tet.2012.05.065.

References and notes

1. (a) Halder, G. J.; Kepert, C. J.; Moubaraki, B.; Murray, K. S.; Cashion, J. D. *Science* **2002**, *298*, 1762; (b) Maspoch, D.; Ruiz-Molina, D.; Wurst, K.; Domingo, N.; Cavallini, M.; Biscarini, F.; Tejada, J.; Rovira, C.; Veciana, J. *Nature Mater.* **2003**, *2*, 190; (c) Niel, V.; Thompson, A. L.; Munoz, M. C.; Galet, A.; Goeta, A. E.; Real, J. A. *Angew. Chem., Int. Ed.* **2003**, *42*, 3760; (d) Cheng, X.-N.; Zhang, W.-X.; Lin, Y.-Y.; Zheng, Y.-Z.; Chen, X.-M. *Adv. Mater.* **2007**, *19*, 1494; (e) Veber, S. L.; Fedin, M. V.; Potapov, A. I.; Maryunina, K. Y.; Romanenko, G. V.; Sagdeev, R. Z.; Ovcharenko, V. I.; Goldfarb, D.; Bagryanskaya, E. G. *J. Am. Chem. Soc.* **2008**, *130*, 2445; (f) Nakabayashi, K.; Ozaki, Y.; Kawano, M.; Fujita, M. *Angew. Chem., Int. Ed.* **2008**, *47*, 2046; (g) Horike, S.; Shimomura, S.; Kitagawa, S. *Nature Chem.* **2009**, *1*, 695; (h) Ohtani, R.; Yoneda, K.; Furukawa, S.; Horike, N.; Kitagawa, S.; Gaspar, A. B.; Munos, M. C.; Real, J. A.; Ohba, M. *J. Am. Chem. Soc.* **2011**, *133*, 8600; (i) Ferrando-Soria, J.; Ruiz-Garcia, R.; Cano, J.; Stiriba, S.-E.; Vallejo, J.; Castro, I.; Julve, M.; Lloret, F.; Amoros, P.; Pasan, J.; Ruiz-Perez, C.; Journaux, Y.; Pardo, E. *Chem.—Eur. J.* **2012**, *18*, 1608.
2. (a) Igarashi, K.; Nogami, T.; Ishida, T. *Chem. Commun.* **2007**, 501; (b) Igarashi, K.; Nogami, T.; Ishida, T. *Polyhedron* **2009**, *28*, 1672; (c) Osada, S.; Igarashi, K.; Nogami, T.; Ishida, T. *Chem. Lett.* **2010**, *39*, 576.
3. Ullman, E. F.; Osiecki, J. H.; Boocock, D. G. B.; Darcy, R. *J. Am. Chem. Soc.* **1972**, *94*, 7049.
4. (a) Kahn, O. *Molecular Magnetism*; VCH: New York, NY, 1993; (b) Gatteschi, D.; Sessoli, R.; Villain, J. *Molecular Nanomagnets*; Oxford University: New York, NY, 2006; (c) Caneschi, A.; Gatteschi, D.; Sessoli, R.; Rey, P. *Acc. Chem. Res.* **1989**, *22*, 392; (d) Ishii, N.; Okamura, Y.; Chiba, S.; Nogami, T.; Ishida, T. *J. Am. Chem. Soc.* **2008**, *130*, 24.
5. (a) Osanai, K.; Okazawa, A.; Nogami, T.; Ishida, T. *J. Am. Chem. Soc.* **2006**, *128*, 14008; (b) Okazawa, A.; Nogami, T.; Ishida, T. *Chem. Mater.* **2007**, *19*, 2733; (c) Okazawa, A.; Nagaichi, Y.; Nogami, T.; Ishida, T. *Inorg. Chem.* **2008**, *47*, 8859.
6. McConnell, H. M. *J. Chem. Phys.* **1910**, *39*, 1910.
7. (a) Tsien, R. Y. *Biochemistry* **1980**, *19*, 2396; (b) Yuchi, A.; Hirai, M.; Wada, H.; Nakagawa, G. *Chem. Lett.* **1990**, *19*, 773; (c) Pethig, R.; Kuhn, M.; Payne, R.; Alder, E.; Chen, T.-H.; Jaffe, L. F. *Cell Calcium* **1989**, *10*, 491.
8. (a) Tanifuji, N.; Irie, M.; Matsuda, K. *J. Am. Chem. Soc.* **2005**, *127*, 13344; (b) Matsuda, K.; Irie, M. *Chem.—Eur. J.* **2001**, *7*, 3466.
9. (a) *Electron Paramagnetic Resonance*; Brustolon, M., Giamello, E., Eds.; Wiley: 2009; (b) Parmon, V. N.; Kokorin, A. I.; Zhidomirov, G. M. *J. Struct. Chem.* **1977**, *18*, 104; (c) Ottaviani, M. F.; Modelli, A.; Zeika, O.; Jockusch, S.; Moscatelli, A.; Turro, N. J. *J. Phys. Chem. A* **2012**, *116*, 174.
10. (a) Nishimaki, H.; Ishida, T. *J. Am. Chem. Soc.* **2010**, *132*, 9598; (b) Kurokawa, G.; Ishida, T.; Nogami, T. *Chem. Phys. Lett.* **2004**, *392*, 74; (c) Matsumoto, S.; Higashiyama, T.; Akutsu, H.; Nakatsuji, S. *Angew. Chem., Int. Ed.* **2011**, *50*, 10879; (d) Kanzaki, Y.; Shiomi, D.; Sato, K.; Takui, T. *J. Phys. Chem. B* **2012**, *116*, 1053; (e) Marsh, D. *J. Mag. Res.* **2008**, *190*, 60; (f) Ishida, T.; Ooishi, M.; Ishii, N.; Mori, H.; Nogami, T. *Polyhedron* **2007**, *26*, 1793.
11. (a) Szydlowska, J.; Pietrasik, K.; Glaz, L.; Kaim, A. *Chem. Phys. Lett.* **2008**, *460*, 245; (b) Parmon, V. N.; Kokorin, A. I.; Zhidomirov, G. M.; Zamaraev, K. I. *Mol. Phys.* **1975**, *30*, 695.
12. (a) Shannon, B. D.; Prewitt, C. T. *Acta Crystallogr., Sect. B* **1969**, *25*, 925; (b) Shannon, B. D. *Acta Crystallogr., Sect. A* **1976**, *32*, 751.
13. Bleaney, B.; Bowers, D. K. *Proc. R. Soc. Lond., Ser. A* **1952**, *214*, 451.
14. Brook, D. J. R.; Yee, G. T.; Hundley, M.; Rogow, D.; Wong, J.; Van-Tu, K. *Inorg. Chem.* **2010**, *49*, 8573.
15. (a) Koide, K.; Ishida, T. *Inorg. Chem. Commun.* **2011**, *14*, 194; (b) Koide, K.; Ishida, T. *Polyhedron* **2011**, *30*, 3034.
16. The EPR line shapes of Ph2bNO and Ph3bNO were deformed in the presence of Sr(hfac)$_2$in toluene, giving the broadening of the second and fourth lines. Similar experiments using Mg(hfac)$_2$ showed no appreciable effect on the line shapes even when the M/L ratio was 5/1
17. (a) Segal, B. G.; Kaplan, M.; Fraenkel, G. K. *J. Chem. Phys.* **1965**, *43*, 4191; (b) Gerson, F.; Jachimowicz, J.; Leaver, D. *J. Am. Chem. Soc.* **1973**, *95*, 6702.
18. Gex, J. N.; Daul, C.; von Zelewsky, A. *Chem. Phys. Lett.* **1986**, *132*, 276.
19. (a) Boyd, S.; Bryson, A.; Nancollas, G. H.; Torrance, K. *J. Chem. Soc.* **1965**, 7353; (b) Delgado, R.; Frausto de Silva, J. J. R.; Vas, M. C. T. A.; Paoletti, P.; Micheloni, M. *J. Chem. Soc., Dalton Trans.* **1989**, 133.
20. No meaningful EPR spectrum change was observed in a similar reaction using water or methanol in place of toluene.
21. (a) Ulrich, G.; Turek, P.; Ziessel, R.; De Cian, A.; Fischer, J. *Chem. Commun.* **1996**, 2461; (b) Ulrich, G.; Turek, P.; Ziessel, R. *Tetrahedron Lett.* **1996**, *37*, 8755.
22. Gutsche, C. D.; No, K. H. *J. Org. Chem.* **1982**, *47*, 2708.
23. (a) Calder, A.; Forrester, A. R. *Chem. Commun. (London)* **1967**, 682; (b) Forrester, A. R.; Hepburn, S. P.; McConnachie, G. *J. Chem. Soc., Parkin Trans. I* **1974**, 2213.
24. CrystalStructure 4.0, Crystal Structure Analysis Package; Rigaku: Tokyo 196-8666, Japan, 2010.